



Cite this: *Nanoscale*, 2020, **12**, 21015

## Leveraging synthetic particles for communication: from passive to active systems

Jiabin Luan, † Danni Wang † and Daniela A. Wilson \*

Received 31st July 2020,  
Accepted 12th October 2020

DOI: 10.1039/d0nr05675h

rsc.li/nanoscale

Communication is one of the most remarkable behaviors in the living world. It is an important prerequisite for building an artificial cell which can be considered as alive. Achieving complex communicative behaviors leveraging synthetic particles will likely fill the gap between artificial vesicles and natural counterpart of cells and allow for the discovery of new therapies in medicine. In this review, we highlight recent endeavors for constructing communication with synthetic particles by revealing the principles underlying the communicative behaviors. Emergent progress using active particles to achieve communication is also discussed, which resembles the dynamic and out-of-equilibrium properties of communication in nature.

### 1. Introduction

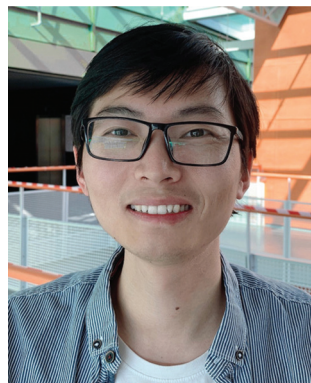
Communication, one of the most fundamental behaviors, is ubiquitous across species at various scales ranging from microscopic cells to macroscopic animals. Although verbal, visual and tactile communications might be easily perceptible, signal transmission especially chemical signals play a central role in communication. For example, bacteria synchronize the

community behaviors and function as multicellular organisms by producing and releasing small molecules termed autoinducers which is known as quorum sensing (QS).<sup>1</sup> Pheromones are secreted by insects and vertebrates for intraspecific communication to attract mates, to trigger alarm, to recognize offspring, and so forth.<sup>2,3</sup> Such exquisite communicative behaviors are naturally evolved and are beneficial for the survival of the species.

The universal communication in nature has stimulated research on realizing communication between engineered cells.<sup>4,5</sup> Building communication through engineering cells started much earlier and progressed more rapidly than using synthetic particles which will be focused in the current review.

*Institute for Molecules and Materials, Radboud University, Heyendaalseweg 135, 6525 AJ Nijmegen, The Netherlands. E-mail: d.wilson@science.ru.nl*

†These authors contributed equally to the work.



**Jiabin Luan**

*Jiabin Luan received his BEng. in Materials Science and Engineering from the University of Science and Technology Beijing and MSc. in Chemistry and Physics of Polymers from Fudan University, Shanghai, in 2013 and 2016, respectively. During his master, he worked on the molecular design of an injectable hydrogel as drug delivery systems for biomedical applications. He returned to the academia after one-year working in industry and started his Ph.D.*

*journey in Prof. Daniela Wilson's group in 2018 focusing on developing a novel nanomotor system using Janus dendrimers.*



**Danni Wang**

*Danni Wang received her BEng. in Macromolecular Science (2016) and MSc. degree in Chemistry and Physics of Polymers (2019) from Fudan University, Shanghai (China). During her master's study, she focused on the design of injectable chemically cross-linking hydrogels for 3D cell culture and drug delivery. Early in 2019, She joined Prof. Roeland Nolte's group as a Junior Researcher and studied the interaction between chiral porphyrin cage compounds (chiral hosts) and viologens (guests). She is now a Ph.D. candidate in Prof. Daniela Wilson's group. Her research interests center upon self-propelled polymeric biocompatible micro/nanomotors for drug delivery.*



Although exploiting cellular communication has been shown to broaden the possibility of synthetic biology and leads to new therapeutic applications,<sup>6</sup> limitations come along with these technologies. Living cells keep growing and evolving which may undermine the engineered pathway as intended.<sup>7</sup> Complex signal pathways inside cells might further obscure the conclusion drawn from the communicative behaviors of cells on a population-wide scale. On the contrary, synthetic particles are usually stable enough to be exempt from the possible evolution like cells. Precise control of the fabrication of synthetic particles offers the possibility to study the complex communicative behaviors by rebuilding the communicative network.

The sophisticated communicative behaviors in nature keeps inspiring the design of synthetic particles to communicate between each other, or between synthetic particles and living cells, or to realize the collective behavior of the synthetic particles. Exciting examples based on synthetic platforms have been recently shown to mimic the communication in nature, ranging from microscopic QS of bacteria to macroscopic collective behaviors of flocking of birds. Designing synthetic particles with communicative ability is not only essential for realizing complex dynamic behaviors, but also beneficial for emergent applications.

To date, synthetic particles involved in artificial communicative study generally fall into two categories, namely passive particles and active particles. Passive particles which are exemplified by classical particles such as liposomes, polymersomes, hydrogel particles and so forth, only exhibit Brownian motion. In contrast, active particles, also named as micro/nanomotors, micro/nanomachines, micro/nanorobots, active Brownian particles, and so forth, can harvest energy of various types to

move autonomously to accomplish tasks in a self-organized way. Different from the passive particles, asymmetry, either in the shape of the particle or the distribution of catalysts, is an essential element for active particles. Fig. 1 shows typical examples of passive and active particles. Detailed introduction of synthetic particles, the fabrication technologies and potential applications are not discussed and can be found in other comprehensive reviews and research.<sup>8–15</sup>

This review focuses on the recent progress of artificial communication using both passive and active particles. Communicative behaviors are defined here as the interaction between different communities of synthetic particles or between synthetic particles and cells. Therefore, examples showing the interaction between synthetic particles and the environment will not be included and readers are directed to other reviews for more information.<sup>16–18</sup> Different from several existing reviews discussing communication between artificial cells,<sup>7,19–22</sup> we set no limit of both the types of synthetic particles and the methods for enabling the communication. The current review is organized by unveiling the principles behind the communicative behaviors using synthetic platforms. To date, most communication studies were established with passive particles. Here we also discussed a few emerging efforts using active particles to demonstrate communicative and collective behaviors, which may bring us closer to mimicking the natural communication as will be further discussed in the following section. An overview of artificial communication leveraging synthetic particles, both passive and active, is shown in Fig. 2. Rather than being comprehensive, we intend to highlight state-of-art principles of leveraging synthetic particles to achieve communication.

## 2. Diffusion mediated communication

Cells typically communicate with each other to organize in space, to regulate gene expression, and to coordinate collective behaviors by using chemical signals such as proteins or other biomolecules. Cell-cell signaling involves the transmission of chemical signals from the sender cells to the receiver cells. Briefly, the sender produces chemical signals that further release into the extracellular environment. Receiver cells can detect the chemical signals and respond in real time. Inspired by nature, researchers have developed various synthetic cell-like architectures to implement communication by means of the diffusion of chemical signals. In the following part, we will discuss the recent progress on the communication models based on two diffusion mechanisms, namely non-specific diffusion and pore-mediated diffusion.

### 2.1 Non-specific diffusion

With respect to the mechanisms of chemical signaling, non-specific diffusion of signals offers a straightforward design to realize artificial communication. This is notably the case for some small molecules such as the QS signal acyl-related homo-



**Daniela A. Wilson**

*Daniela A. Wilson (born Apreutesei) received her Ph.D. with distinction “summa cum laude” from Gheorghe Asachi Technical University of Iasi, Romania in 2007. During her Ph.D. she obtained two fellowships in Japan and the U.K. as an exchange Ph.D. student and Marie Curie fellow. She then worked as a postdoctoral researcher at University of Pennsylvania, Philadelphia, USA, and Radboud University,*

*Nijmegen, Netherlands, in the groups of Prof. Virgil Percec and Prof. Roeland Nolte. She is currently Professor of Systems Chemistry at the Institute for Molecules and Materials, Radboud University, Nijmegen, The Netherlands. Her research interests focus on the design of intelligent, self-propelled, and self-guided supramolecular assemblies and their communication and interaction as next generation nanoengineered delivery systems.*



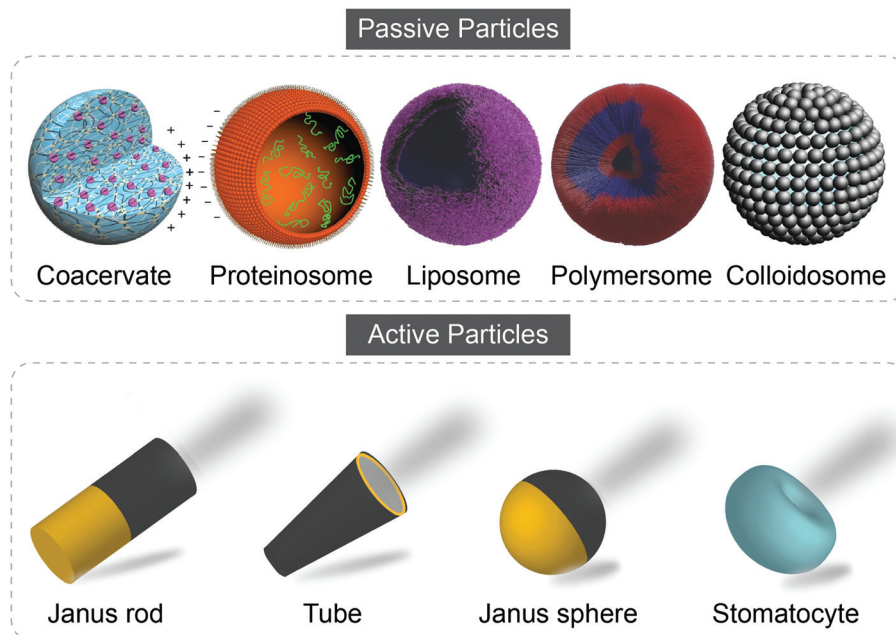


**Fig. 1** Representative examples of passive and active particles. Figures reproduced with permission: coacervate and proteinosome from ref. 55, Copyright 2017 Springer Nature; liposome and polymersome from ref. 8, published by The Royal Society of Chemistry; colloidosome from ref. 50, Copyright 2017 Springer Nature.

serine lactones (AHLs) or glucose. Based on the free transmembrane diffusion of these small molecules, researchers applied different strategies including signaling cascade reactions or genetic circuits to endow the synthetic particles with the capabilities to communicate with each other or with living cells.

**2.1.1 Signaling cascade.** Signaling cascades play a role in communication by means of non-specific diffusion. This strategy involves a series of chemical reactions where successive stage processes the output of the preceding one. Glucose oxidase (GOx) and its substrate glucose are the most favorable candidates.

By triggering the enzymatic reaction, Mann group achieved one-way signaling communication between GOx-containing silica colloidosomes and alkaline phosphatase (ALP)-containing clay colloidosomes (Fig. 3A).<sup>23</sup> The chemical input glucose was decomposed by GOx in silica colloidosomes, producing hydrogen peroxide ( $\text{H}_2\text{O}_2$ ) signal which further diffused out and initiated a self-directed polymerization at the surface of clay colloidosomes. This endowed the colloidosomes with a temperature-responsive poly(*N*-isopropylacrylamide) (PNIPAM) wall, leading to well-controlled membrane permeability by tuning the temperature. In this work, the researchers fabricated a primitive communication model with functional activation between two different inorganic populations.

Relying on the same glucose-GOx enzymatic reaction, Raghavan and coworkers developed “killer” microcapsules that can selectively destroy target microparticles in the vicinity (Fig. 3B).<sup>24</sup> “Killer” microcapsule were obtained by encapsulating the enzyme GOx in chitosan microcapsules. Gluconate

ions were formed after the chemical input glucose diffused inside. Subsequently, ions would diffuse into the target alginate beads in the vicinity, chelate away the  $\text{Cu}^{2+}$  and cause the degradation of the target beads. The study provides a primitive imitation of immune systems, where killer T cells destroy the infected cells.

In addition to the one-way communication, Llopis-Lorente *et al.* achieved cargo delivery *via* two-way interactive communication between two enzyme-powered Janus nanoparticles (Fig. 3C).<sup>25</sup> The authors designed Janus Au-mesoporous silica gated nanoparticles with two faces. A mesoporous face was loaded with a cargo and capped with stoppers ( $\beta$ -cyclodextrin ( $\beta$ -CD):benzimidazole complex), and the opposite Au face was functionalized with different biomolecules ( $\beta$ -galactosidase ( $\beta$ -Gal) and GOx). The interactive communication was launched by the addition of input (lactose). First, the sender functionalized with  $\beta$ -Gal hydrolyzed the lactose to glucose (messenger 1). Afterwards, glucose received by the receiver functionalized with GOx was transformed to gluconic acid. This reaction led to a local pH drop, thus causing the de-threading of  $\beta$ -CD:benzimidazole and the following release of cargo *N*-acetyl-L-cysteine (messenger 2). Finally, the sender responded to the feedback with the rupture of the disulfide linkages and the release of chemical output  $(\text{Ru}(\text{bpy})_3)^{2+}$ . Through a series of careful design, the authors showed a reciprocal cross-talking between the binary populations. Later, the same group extended the interactive communication from particle and particle to particle and yeast cells.<sup>26</sup> Here the sender changed to be yeast cells, while the receiver particles remained the same except the encapsulated cargo became genotoxic



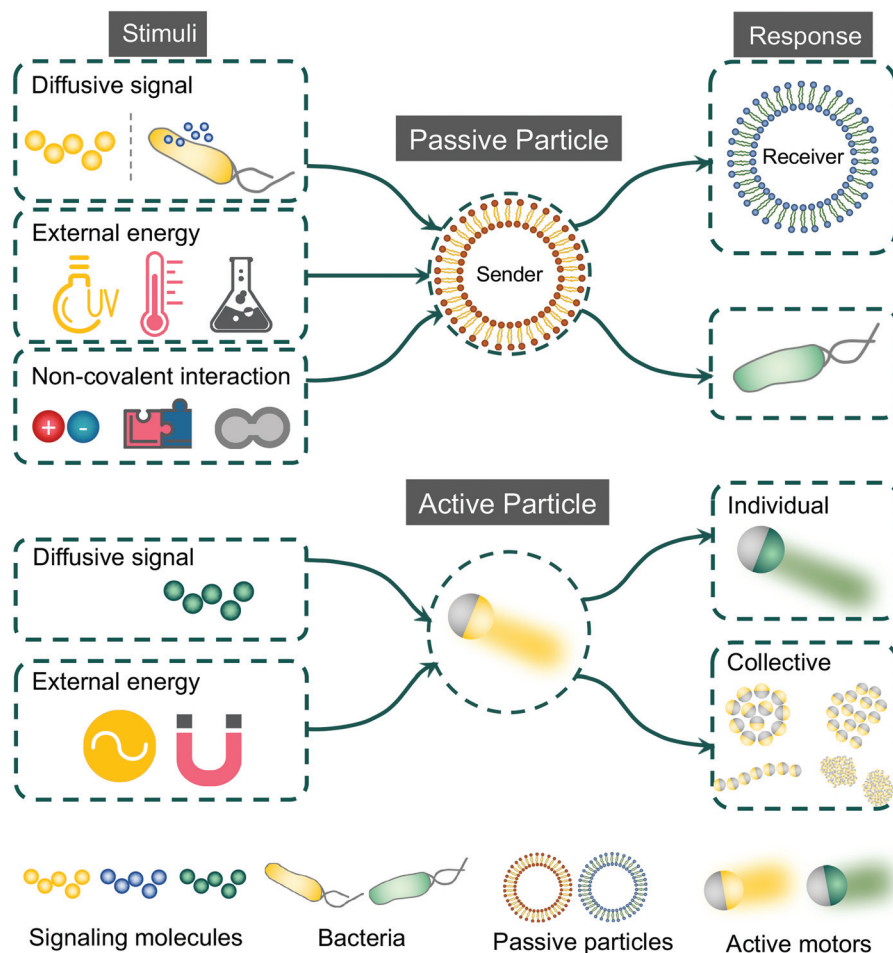


Fig. 2 Overview of artificial communication accomplished synthetically with passive and active particles.

phleomycin. External addition of sucrose was converted to glucose and fructose by yeast cells. Similar to previous example, glucose triggered the release of encapsulated phleomycin from the receiver as a feedback message to the sender cells, leading to the production of fluorescence. Very recently, the group reported an interesting ternary communication among nanoparticle–cell–nanoparticle to induce apoptosis in cancer cells (Fig. 3D).<sup>27</sup> First community of mesoporous particles were loaded with 9-*cis*-retinoic acid and capped with interferon- $\gamma$ . Both molecules were able to induce expression of TLR3 in SK-BR-3 breast cancer cells. On the other hand, the second population of particles were capped with a synthetic dsRNA agonist of TLR3, polyinosinic–polycytidylic acid, which was known to induce apoptosis of cancer cells. Benefited from the upregulated expression of TLR3, the interaction of the second type of particles with cancer cells was enhanced, leading to cell death. This proof-of-concept work shows a strategy of exploiting two communities of synthetic particles to work cooperatively to inhibit the growth of cancer cells.

**2.1.2 Genetic circuits.** Living cells evolve complex genetic networks to communicate with the community. Utilizing the tools of synthetic biology, genetic circuits have also been con-

structed to realize the communication between synthetic particles, or synthetic particles and cells. Genetic circuits are assemblies of unnatural DNA segments encoding protein or RNA that enable cells to interact with each other to perform multiple functions. Many groups exerted efforts to involve cell or cell-free genetic circuits in synthetic particles to demonstrate the communication.

For example, sender–receiver bacterial system containing genetic circuits was included within microemulsion droplets, and it was illustrated that engineered sender bacteria in one droplet could communicate with receiver bacteria in neighboring droplet.<sup>28</sup> In this system, the sender bacteria synthesized *N*-(3-oxo-hexanoyl)-L-homoserine lactone (3OC6HSL) signal which would diffuse into the environment. The receiver bacteria responded to this QS signal with expression of green fluorescent protein (GFP). In addition, an AND-gate gene circuit was built by integration of both 3OC6HSL and conventional inducer isopropyl- $\beta$ -D-thiogalactopyranoside (IPTG). The gene expression in receiver bacteria was switched on only when reservoir droplets with both input signals were present.

By constructing cell-free genetic circuits within a giant liposome, Stano group generated a synthetic cell capable of com-



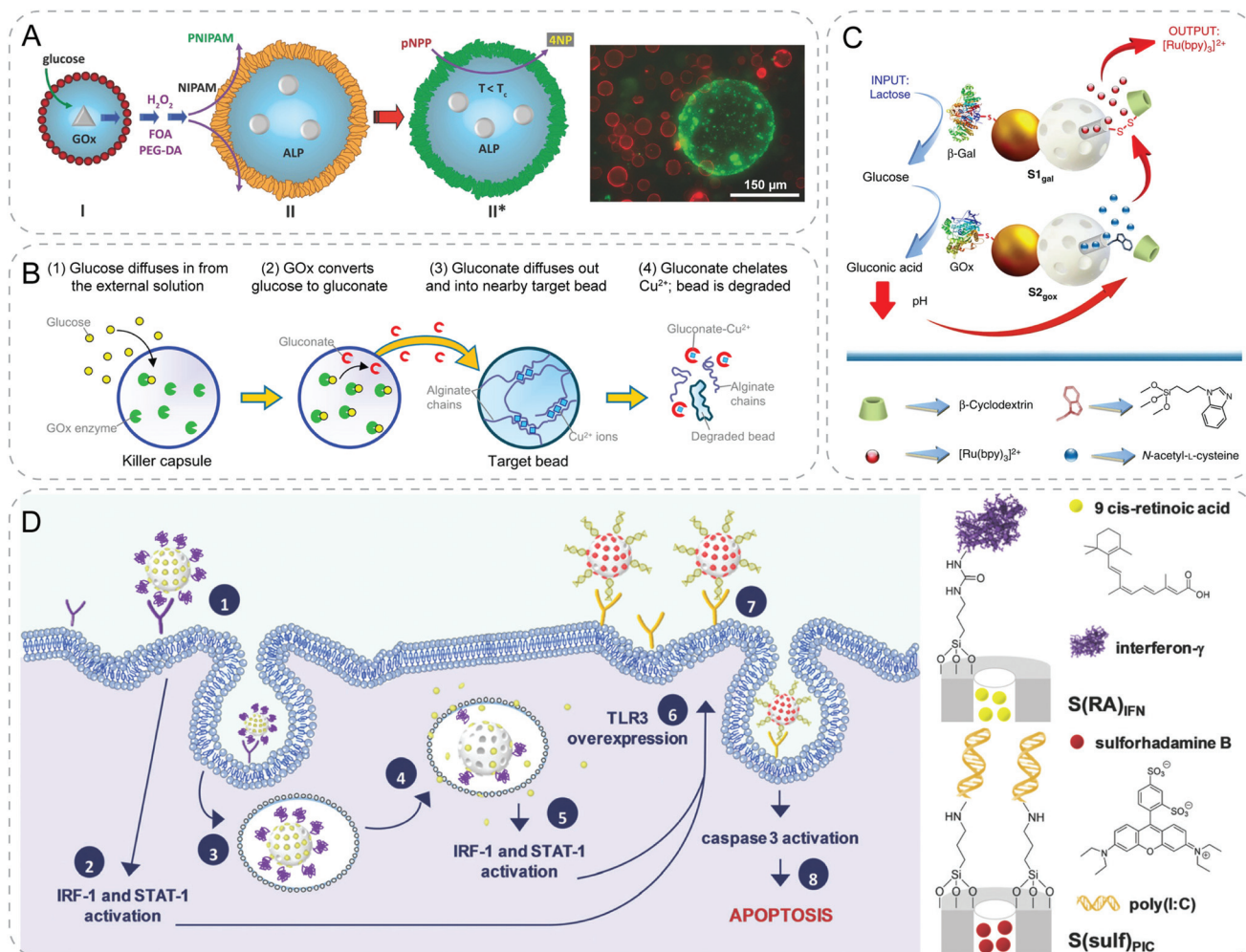


**Fig. 3** Communicative behaviors mediated by non-specific diffusion based on signaling cascades. (A) Glucose/glucose oxidase (GOx) cascade mediated the polymerization of the *N*-isopropylacrylamide (NIPAM) shell of the other colloidosome. Consequently, enzyme activity within the PNIPAM-colloidosome is gated by the temperature-responsive PNIPAM membrane.<sup>23</sup> (B) Artificial killing process. GOx inside the killer capsule produces gluconate ions by catalyzing external glucose, which further diffuses into the target bead in vicinity. The gluconate ions then chelate away the cross-linking  $\text{Cu}^{2+}$  cations of the alginate bead, leading to its degradation.<sup>24</sup> (C) Interactive communication between Janus particles. Chemical input, lactose, is hydrolyzed by  $\beta$ -galactosidase ( $\beta$ -Gal) on the sender ( $\text{S1}_{\text{gal}}$ ) to generate glucose, which is oxidized by GOx into gluconic acid on the receiver ( $\text{S2}_{\text{gox}}$ ). The presence of acid drops the local pH, resulting in the de-threading of the stopper,  $\beta$ -cyclodextrin:benzimidazole complex and release of cargo *N*-acetyl-L-cysteine. The released molecule acts as the feedback signal to trigger the delivery of  $[\text{Ru}(\text{bpy})_3]^{2+}$  reporter from  $\text{S1}_{\text{gal}}$ .<sup>25</sup> (D) Ternary communication from nanoparticle to cell to nanoparticle. Particle 1,  $\text{S}(\text{RA})_{\text{IFN}}$ , releases 9-*cis*-retinoic acid and interferon- $\gamma$  after the endocytosis and enhances the overexpression of membrane TLR3 receptors. Afterwards, particle 2,  $\text{S}(\text{sulf})_{\text{PIC}}$ , is internalized more effectively to induce cell apoptosis.<sup>27</sup> Figures reproduced with permission from: (A), ref. 23, Copyright 2016 John Wiley and Sons; (B), ref. 24, Copyright 2016 American Chemical Society; (C), ref. 25, Copyright 2017 Springer Nature; (D), ref. 27, Copyright 2020 Royal Society of Chemistry.

communicating with bacteria.<sup>29</sup> *Pseudomonas aeruginosa* was engineered as the receiver bacteria which contained a genetic reporter device for *N*-butanoyl-L-homoserine lactone (C4-HSL)-induced bioluminescence. Signal molecule C4-HSL was synthesized by synthase RhlI inside the vesicles. The molecules diffused out through the lipid membrane freely. Once the signal molecule reached the engineered bacteria *Pseudomonas aeruginosa*, it would bind to the receptor RhlR within the engineered bacteria and in turn emit bioluminescent output.

Natural organelles such as mitochondria, or endosomes are composed of multicompartments where diverse chemical com-

munication takes place under highly regulated conditions. Raghavan group demonstrated chemical communication mediated by non-specific diffusion between different compartments within vesicles (Fig. 4A).<sup>30</sup> Artificial cells with several compartments were fabricated using water-gas microfluidic technology. Distinct strains of bacteria could be easily encapsulated in different compartments of the alginate/chitosan microcapsules. The signal from one bacteria strain would diffuse out and into the neighboring compartment, then the other bacteria strain would respond to this signal thus generating fluorescent output.



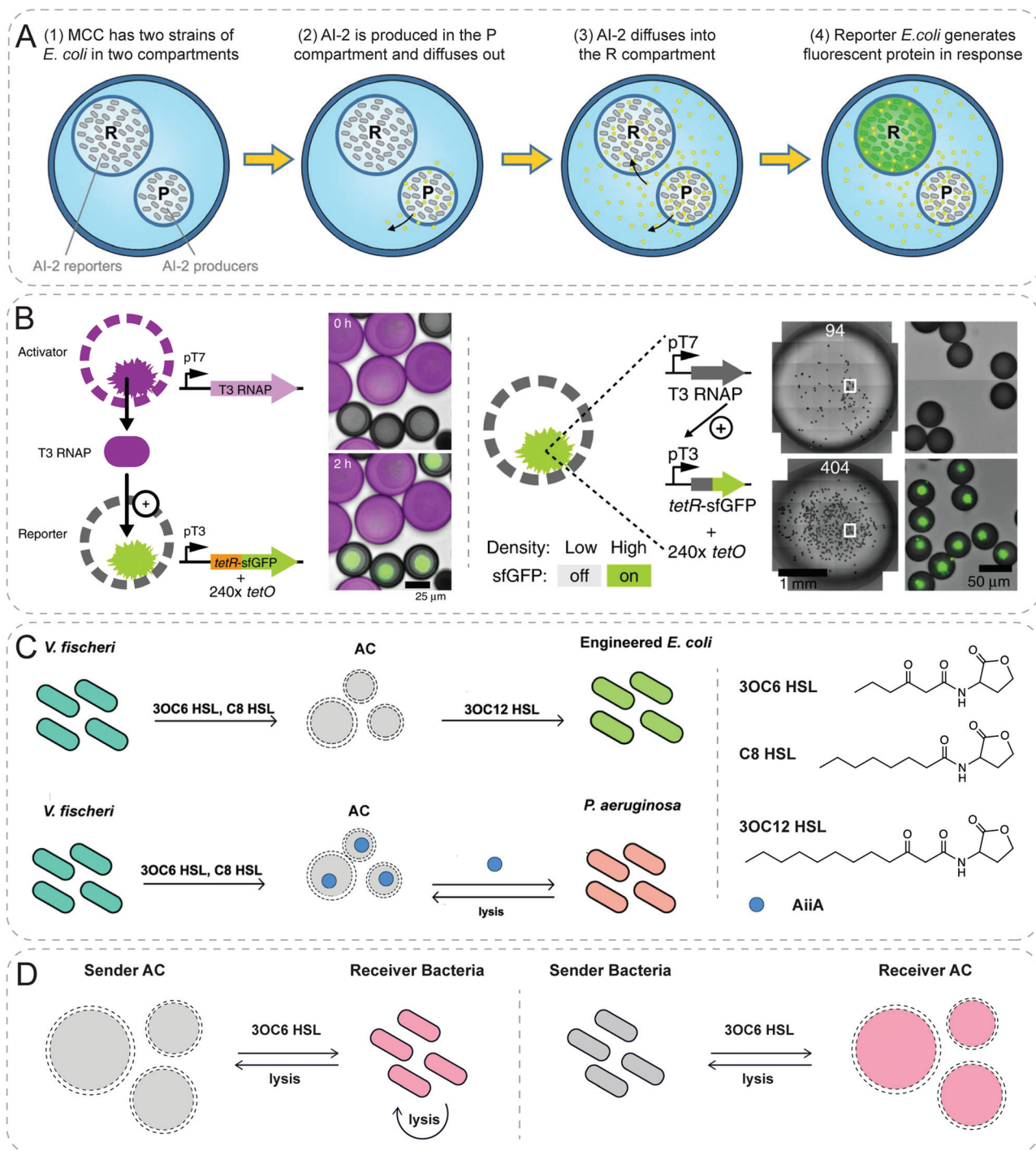


**Fig. 4** Communicative behaviors mediated by non-specific diffusion based on genetic circuits. (A) Compartmentalized bacterial cascade communication. Two distinct strains of *E. coli* are encapsulated inside a multicompartment capsule (MCC). Autoinducer 2 (AI-2) is produced and diffuses from one strain in P compartment to the other strain in R compartment, where the reporter bacteria generate fluorescence in response.<sup>30</sup> (B) Diffusive communication and density sensing using cell-mimics with artificial nuclei. T3 RNA polymerase (T3 RNAP) as the diffusible signaling molecule is synthesized within the activator particles. The reporter particles respond to the signal and express the fluorescent protein in the hydrogel nuclei (left). At low density with only 94 particles of each droplet, there is no fluorescence, while at high density with more than 400 particles, reporters show fluorescent response. This population-density responsive behavior mimics the quorum sensing (right).<sup>31</sup> (C) Two-way communication between artificial and natural cells. Artificial cell (AC) mediates communication between two different bacteria by sensing quorum signal from *V. fischeri*, followed by synthesizing signals for *E. coli*. Furthermore, AC is engineered to sense *V. fischeri* and in response to degrade quorum signals of *P. aeruginosa* through releasing enzyme AiiA after degradation.<sup>34</sup> (D) Negative feedbacks between AC and bacteria. AC sends signal to bacteria leading to the lysis of bacteria, which ruptures the AC as a negative feedback response (left). *Vice versa*, bacteria send signal to AC which generates a toxicant to kill the bacteria (right).<sup>35</sup> Figures reproduced with permission from: (A), ref. 30, Copyright 2017 Royal Society of Chemistry; (B), ref. 31, Copyright 2018 Springer Nature; (C), ref. 34, Copyright 2017 American Chemical Society; (D), ref. 35, Copyright 2018 American Chemical Society.



As presented in the previous section, signaling molecules for communication between synthetic particles have been limited to small molecules so far. Devaraj and colleagues creatively designed cell-mimics capable of communicating with neighboring populations through diffusive protein molecules and displaying collective behavior similar to bacterial quorum sensing (Fig. 4B).<sup>31</sup> In this work, they built porous synthetic particles with permeable polymer membrane (diameter 200–300 nm) and a clay-DNA hydrogel nuclei containing the transcription machinery. To demonstrate the communication, a two-stage activation cascade was constructed. Upon transcription and translation, T3 RNA polymerase (T3 RNAP) as the diffusive signaling molecule would be synthesized within the activator particles. The reporter particles would respond to the signal and express the fluorescent protein. In addition, the particles containing both the activation and reporter circuits would present a collective behavior where fluorescence accumulated in particles only at high densities. At low densities, the release of T3 RNAP from the hydrogel nuclei could not be detected due to its low concentration. The escalation of densities resulted in sufficient T3 RNAP which was able to induce the expression of the reporter.

More complex communicative behaviors were realized using microparticles whose surfaces were decorated with enzyme-driven DNA circuits.<sup>32</sup> The particles could communicate with and also sense the signals from the neighbors through signal diffusion. In a large population of particles, the collective behaviors of individual particles resulted in propagation of chemical information over a distance of three orders of magnitude larger than the particles themselves. Later, instead of grafting on the surface, DNA circuits were encapsulated in proteinosomes with semipermeable membranes to protect them from nuclease digestion.<sup>33</sup> A variety of population behaviors were also demonstrated such as cascaded amplification, bidirectional communication and distributed computing.

Furthermore, by building genetic constructs within lipid vesicles, Mansy group successfully achieved two-way chemical communication between bacteria and artificial cells that are able to both sense and synthesize QS signaling molecules (Fig. 4C).<sup>34</sup> Through rebuilding corresponding genetic constructs *in vitro* within phospholipid vesicles, resultant artificial cells could synthesize quorum molecules and send them to various strains of bacteria, such as *V. fischeri*, *V. harveyi* and *E. coli*, respectively. In addition, these artificial cells could mediate communication between two different bacterial species. After sensing the quorum molecules produced from *V. fischeri*, the genetic device of the artificial cells could synthesize the other quorum molecule in response which could be further sensed by a different strain of bacteria *E. coli*. Interestingly, the genetic device inside the artificial cell could also be designed to degrade quorum signals of *P. aeruginosa* after sensing *V. fischeri*. Although more work is required, the study shows potential in using artificial cells to interfere quorum signals of bacteria, which might be beneficial to inhibit the formation of biofilm. Notably, a cellular Turing test

was further carried out to quantify how similar artificial cells can imitate natural cells. Although the final calculation of the similarity was exaggerated as admitted by the authors, this work gave the first step to quantitatively show the gap between artificial cells and the living counterparts.

Subsequently, another representative work from Tan group also illustrated a two-way feedback response between synthetic particles and bacteria (Fig. 4D).<sup>35</sup> By encapsulating synthetic gene networks into liposomes, a negative feedback response between artificial cells and bacteria was demonstrated. Briefly, the chemical signal AHL synthesized by synthase *EsaI* in the sender artificial cells was detected by the receiver bacteria. In response, the bacteria expressed peptide Bac2A which killed the sender bacteria themselves and ruptured the sender artificial cells consequently. A reverse negative feedback was also established by switching the genetic networks inside artificial cells and bacteria. In this scenario, artificial cells sensed the AHL produced by bacteria followed by the synthesis of Bac2A. Bac2A diffused out through the membrane and killed the bacteria.

Despite the huge potential, the specific design of genetic circuits remains one of the most challenging aspects. In addition to the sensitivity to environment and the difficulty of screening in directed-evolution, genetic circuits require the precise balancing of the complex regulatory elements which are technically challenging.<sup>36</sup> Recent studies mostly relied on a fluorescent reporter to quantify the performance of genetic circuits. However, the degradation rates of fluorescent protein would limit the dynamic measurements, thus making the long-time scale tracking on communication virtually impossible. Meanwhile, the averaged fluorescence output among the populations failed to account for individual differences which might lead to inconclusive results.

**2.1.3 Others.** By implementing different affinities of the formation of DNA duplex, chemically programmed communication was shown between two hierarchically assembled coacervate protocells.<sup>37</sup> Upon the addition of fuel strand, fuel strand would displace the Cy5-reporter from Cy3/Cy5 colocalization, which further diffused out through the semipermeable membrane of coacervates. Then neighboring coacervate containing FAM-labeled nanoscaffold 2 could capture Cy5-reporter because of a higher affinity, completing the communication between two populations.

## 2.2 Pore mediated diffusion

The non-specific diffusion of signaling molecules is dependent on the membrane permeability of synthetic particles, which limits the range of materials being employed. To bypass the low permeability of membranes, membrane-spanning pores generated by alpha-hemolysin ( $\alpha$ -HL) protein is an effective solution. This broadens the toolbox of both the signaling molecules and the synthetic materials for establishing communication.

**2.2.1 Signaling cascade reactions.** GOx-horseradish peroxidase (HRP) cascade reaction is one of the most common enzyme cascade reactions being introduced to achieve com-



munication. For instance, a gene-directed chemical communication pathway between lipid vesicles and proteinosomes was built on this cascade.<sup>38</sup> The influx of 3OC6HSL from the environment to lipid vesicles induced cell-free gene expression of  $\alpha$ -HL and membrane pores formation, which in turn assisted the efflux of glucose. As a result, glucose was oxidized at the surface of GOx-PNIPAM proteinosomes to generate H<sub>2</sub>O<sub>2</sub>, which converted Amplex Red to a red fluorescent read-out resorufin in the presence of HRP.

A more complex example was also shown by an engineered three-step enzymatic pathway in multi-compartment liposomes (Fig. 5A).<sup>39</sup> Different enzymes were located in distinct compartments. Substrates and products were diffused through compartments with the help of pores produced from  $\alpha$ -HL. To start, the chemical input lactose diffused into the first compartment and was transformed into D-glucose in the presence of lactase. The generated D-glucose traversed through the bilayer to initiate a subsequent reaction within the second compartment, producing H<sub>2</sub>O<sub>2</sub> in the presence of GOx. When H<sub>2</sub>O<sub>2</sub> diffused into the third compartment, Amplex Red was transformed into the fluorescent product resorufin by HRP.

**2.2.2 Genetic circuits.** As shown in section 2.1.2, genetic circuits displayed great potential in constructing communication between synthetic particles and living cells. This potential could be further increased in the presence of pore-formation by enabling other signaling molecules for communication.

Boyden group engineered synthetic minimal cells including multicomponent genetic circuits and regulatory cascades in a modular design and demonstrated complex cascade communications between multiple populations (Fig. 5B).<sup>40</sup> The sender liposomes were loaded with isopropyl- $\beta$ -D-thiogalactoside (IPTG) and arabinose-inducible gene for  $\alpha$ -HL. Arabinose, supplied externally, permeated into the sensor liposome, and activated chemical inducers arabinose by expressing  $\alpha$ -HL channels. Subsequently, the impermeable IPTG had access to diffuse out with the aid of the produced protein pore and triggered a fluorescent response in the reporter liposome.

Simmel group fabricated a network of droplet-based artificial cells separated by droplet interface bilayers, and built gene circuits within the compartments to implement biomimetic signaling and differentiation processes (Fig. 5C).<sup>41</sup> The researchers achieved communication between the sender and receiver by building a variety of biomimetic circuits. For example, amplified leaky transcription of promoter led to the formation of  $\alpha$ -HL pores and created a positive feedback loop on pore formation *via* arabinose influx. Thereafter chemical input diffused into the neighboring receiver cell with the aid of protein pores and led to differentiation based on environmental information.

Mansy group reported the first synthetic system capable of translating unrecognized signals into a chemical language that bacteria can recognize (Fig. 5D).<sup>42</sup> They engineered the lipid vesicles with IPTG, DNA and transcription-translation machinery. The resultant artificial cells could act as chemical translators by detecting theophylline molecules which could not be

recognized by bacteria, and in turn releasing IPTG which could induce a response in *E. coli*. The authors showed a smart design to employ synthetic particles as a bridge to expand the sensory capabilities of *E. coli*.

**2.2.3 Others.** Efforts to build communication between synthetic particles and living cells mainly relied on genetic circuits adapted from nature. Davis group reported the first pioneering example of QS-like communication between artificial cells and live bacteria by means of the autocatalytic sugar-synthesizing formose reaction (Fig. 6A).<sup>43</sup> The authors encapsulated the precursors of the formose reaction inside liposomes. Notably, to circumvent the incompatibility with the synthesis of the vesicles, the required catalyst calcium hydroxide was formed *in situ* by adding external alkali to vesicles containing soluble but internally trapped calcium ions. Upon the increased pH outside the vesicle, a rise of internal pH drove the formose interaction to produce carbohydrates which diffused out through  $\alpha$ -HL membrane pore and generated carbohydrate-borate complexes outside. These complexes possessed similar structure to the QS signal molecule autoinducer-2, which was able to be sensed by bacterium *Vibrio harveyi* with a bioluminescent response.

3D printing technology was exploited to fabricate a tissue-like material with multi-microcompartments by printing droplet networks containing tens of thousands of heterologous picoliter droplets (Fig. 6B).<sup>44</sup> Microcompartment in networks containing  $\alpha$ -HL membrane pores allowed rapid electrical communication following a specific pathway. In addition, osmosis induced macroscopic self-folding behavior was shown in the printed droplet network. Joining two strips of droplets of different osmolarities would lead to the diffusion of water. Subsequently, swelling and shrinking happened cooperatively in respective populations of droplets, which resulted in the transition from rectangular to circular network.

By integrating the formation of double channels in a nested vesicle system, a synthetic mechanosensitive signaling pathway was recently reported (Fig. 6C).<sup>45</sup> The nested vesicle system was formed by emulsion phase transfer, where inner vesicles containing mechanosensitive protein, MscL, were enclosed by outer giant vesicles with  $\alpha$ -HL. External calcium signals diffused in vesicle lumen through  $\alpha$ -HL pore, and activated a calcium-dependent enzyme, secretory phospholipase A2 (sPLA<sub>2</sub>). MscL responded to the product of sPLA<sub>2</sub> by opening to form pores in the bilayer of the inner vesicle, through which encapsulated calcein released and emitted fluorescence.

### 3. External energy mediated communication

Diffusion mediated communication, although straightforward, usually lacks the possibility to spatiotemporally control the communicative behaviors in demand. External stimuli such as light, temperature and addition of chemicals were introduced





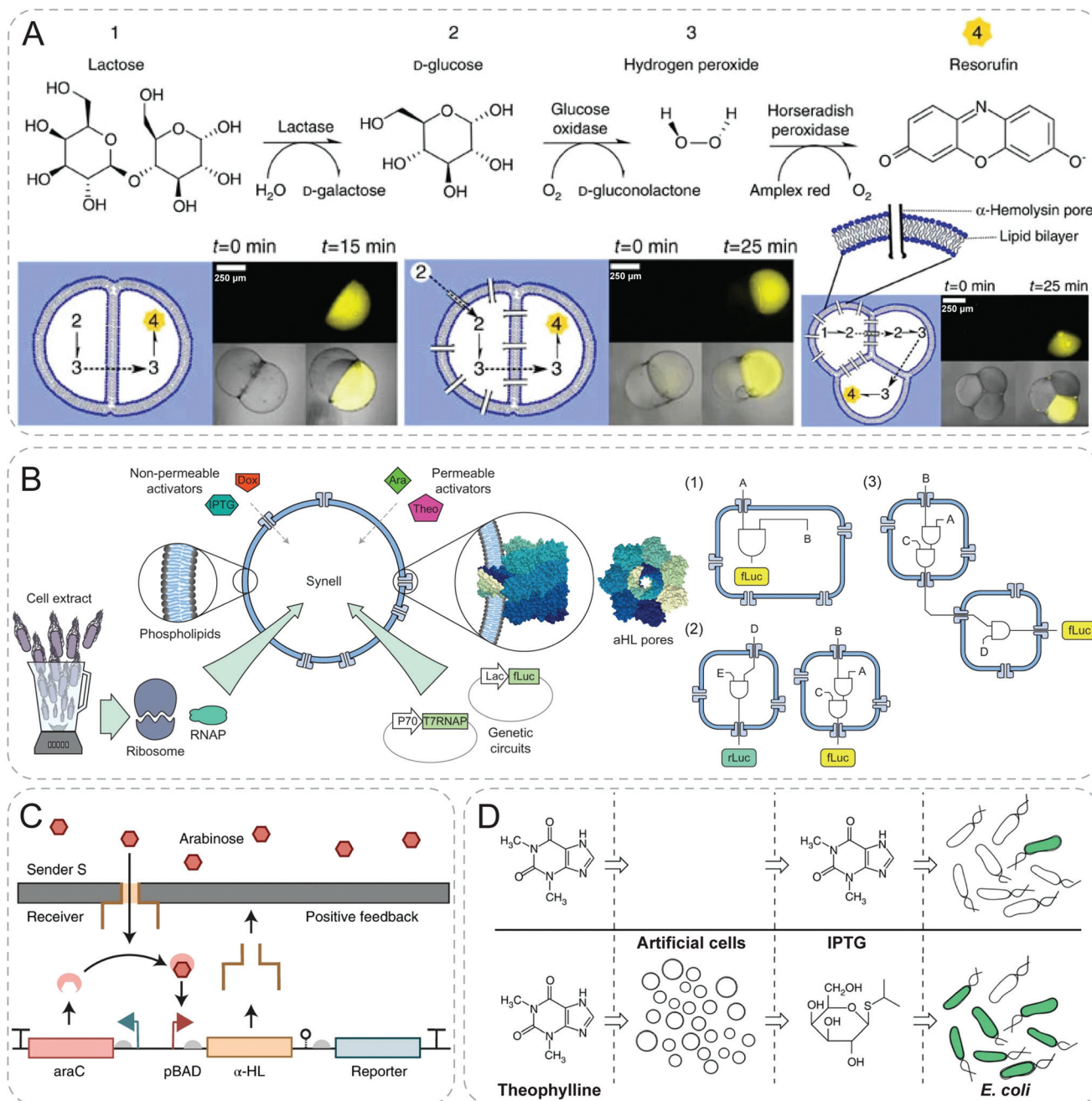


**Fig. 5** Communicative behaviors mediated by pore-assisted diffusion based on signaling cascades or genetic circuits. (A) Multi-step enzymatic cascade reactions with a combination of lactase, glucose oxidase and horseradish peroxidase (HRP). With the aid of transmembrane alpha-hemolysin ( $\alpha$ -HL) pores, fluorescence is generated as an output signal through a series of diffusion of substances from preceding reactions.<sup>39</sup> (B) Modular design of genetic circuit interactions within and between synthetic cells (Synells). Selective permeability of phospholipid membranes allows the permeation of activators, either through direct diffusion or through  $\alpha$ -HL pores. These Synells, together, can be used to create complex modular genetic circuits (1), to function in parallel (2) and to interact with each other (3).<sup>40</sup> (C) Positive feedback response design to mimic signaling and differentiation. Leaky transcription of promoter leads to formation of  $\alpha$ -HL pores of the receiver, which enables the diffusion of arabinose from the sender. Arabinose amplifies the pore expression, creating a positive feedback.<sup>41</sup> (D) Signal translation from artificial cells for *E. coli*. Artificial cells can detect signal molecules, theophylline, and release isopropyl- $\beta$ -D-thiogalactopyranoside (IPTG) which can be sensed by *E. coli*.<sup>42</sup> Figures reproduced with permission from: (A), ref. 39, Copyright 2014 Springer Nature; (B), ref. 40, Copyright 2017 Springer Nature; (C), ref. 41, Copyright 2019 Springer Nature; (D), ref. 42, Copyright 2014 Springer Nature.

to trigger the communication. Alternative methods such as optical tweezers and acoustic standing wave were also able to initiate the communication. It is worth noting that in par-

ticular examples, communication could be reversibly turned on/off under the trigger of external stimulation which provides a precise control of the communication.



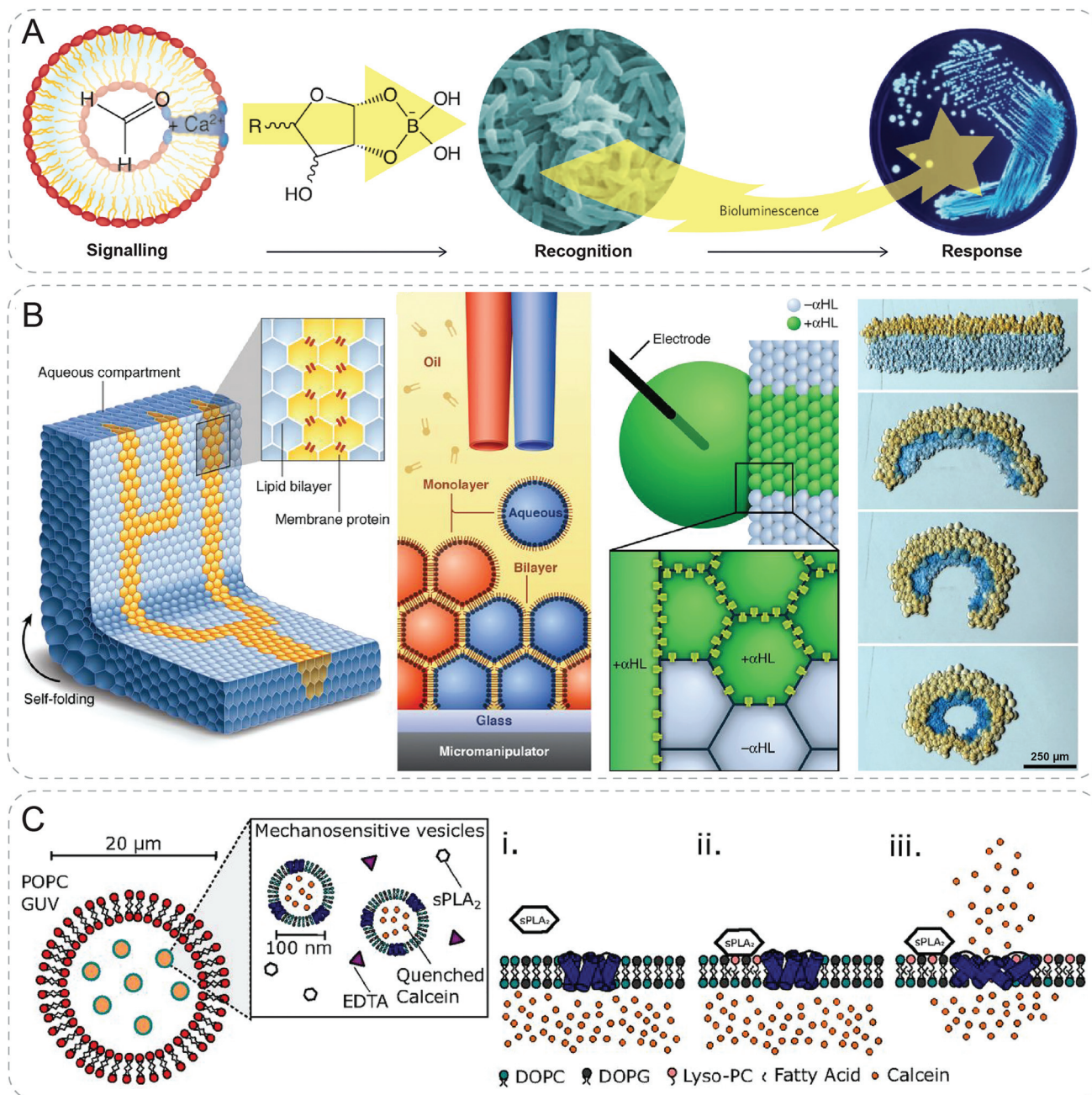


**Fig. 6** Communicative behaviors mediated by pore-assisted diffusion based on other approaches. (A) Synthetic vesicles talk with bacteria by producing sugar molecules. Formose reaction converts formaldehyde to complex sugar molecules which combines with borate after diffusing into the environment. The borate-sugar complex is then sensed by bacterium *V. harveyi* which gives a bioluminescent response.<sup>43,46</sup> (B) 3D-printed droplet network capable of electrical communication and macroscopic self-folding driven by osmosis.<sup>44</sup> (C) Nested artificial cell showing mechanosensitive signaling pathway. Mechanosensitive protein, MscL, in the membrane of inner lipid vesicles is triggered to form pores by secretory phospholipase A2 (sPLA<sub>2</sub>), leading to the release of fluorescent calcein signal.<sup>45</sup> Figures reproduced with permission from: (A), ref. 46, Copyright 2009 Springer Nature; (B), ref. 44, Copyright 2013 AAAS.

### 3.1 Stimuli trigger

**3.1.1 Light.** By introducing light-activated entities to DNA promoter, Booth *et al.* enabled communication between synthetic vesicles through pore formation under the activation of light (Fig. 7A).<sup>47</sup> A light-activated T7 promoter with photoclea-

vable 2-nitrobenzyl groups was placed upstream of genes of interest for further transcription. The promoter bound to multiple monovalent streptavidins through biotin-avidin interaction which blocked the access of T7 RNA polymerase in inactivated state. Upon UV light cleavage of the linkers, T7 RNA polymerase could transcribe the downstream genes. By placing



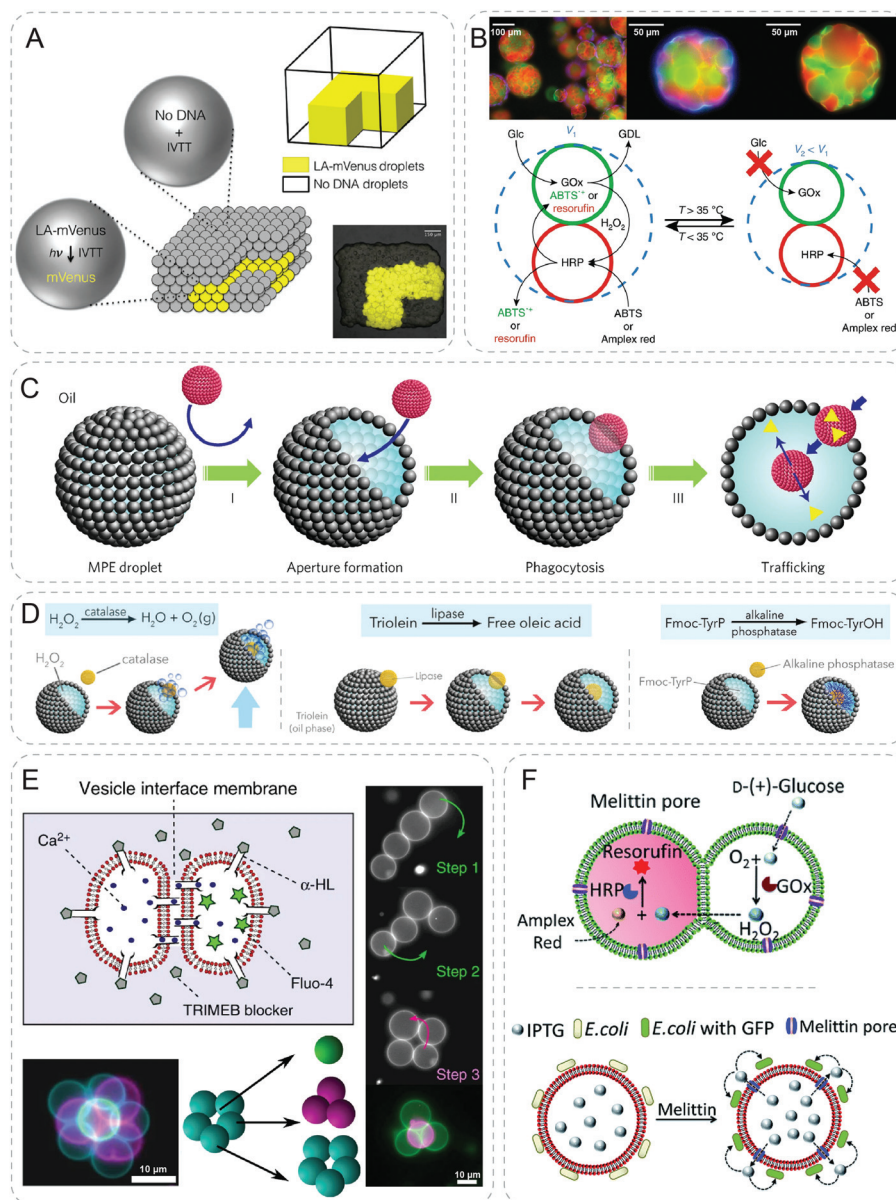


**Fig. 7** Communicative behaviors mediated by external energy. (A) Light-activated patterned expression of mVenus in a 3D-printed synthetic tissue. Upon UV light cleavage of the inhibitor, mVenus-DNA is activated (LA-mVenus) to induce *in vitro* transcription and translation (IVTT), producing yellow fluorescent mVenus protein.<sup>47</sup> (B) Prototissue spheroids capable of mechanochemical transduction of enzyme cascade reactions. In relaxed state ( $V_1$ ), substrates such as glucose (Glc), and 2,2'-azino-bis(3-ethylbenzothiazoline-6-sulfonic acid) (ABTS) or Amplex red diffuse freely through the system, and are converted to D-glucono-1,5-lactone (GDL) and green ABTS<sup>+</sup> or red fluorescent resorufin, respectively by the GOx/HRP cascade reactions. As temperature increases, the cascade reaction is shut down as the system turns to contracted state ( $V_2$ ).<sup>49</sup> (C) Chemical addition induced phagocytosis behavior between synthetic particles. Addition of oleic acid to the oil phase forms an aperture in the magnetic Pickering emulsion (MPE) droplets. Consequently, silica colloidosomes (red objects) are ingested inside the MPE droplet followed by the release of payloads (yellow triangles).<sup>50</sup> (D) Higher-order behaviors based on the same principle of artificial phagocytosis in (C), such as buoyant motion through decomposition of  $H_2O_2$  by catalase, membrane reconstruction through hydrolysis of triolein by lipase, and *in situ* hydrogelation through self-assembly of *N*-fluorenylmethylloxycarbonyl-tyrosine (FmocTyrOH) by alkaline phosphatase.<sup>51</sup> (E) Inter-vesicle communication is mediated by the  $Ca^{2+}$  signal diffusion through  $\alpha$ -HL pores at the interface. Vesicle networks with different geometries are assembled by optical tweezer.<sup>52</sup> (F) Communication between trapped entities using acoustic standing wave. GOx/HRP cascade reaction is realized through signal diffusion between a hemi-fused heterogeneous pair of acoustically trapped vesicles (top). Isopropyl- $\beta$ -D-thiogalactopyranoside (IPTG) diffuses out from the vesicle and triggers the fluorescent response of the co-trapped *E. coli* (bottom).<sup>54</sup> Figures reproduced with permission from: (A), ref. 47, Copyright 2016, the authors; (B), ref. 49, Copyright 2018 Springer Nature; (C), ref. 50, Copyright 2017 Springer Nature; (D), ref. 51, Copyright 2019 The Authors; (E), ref. 52, under a Creative Commons licence CC BY 4.0; (F), ref. 54, published by The Royal Society of Chemistry.



genes of membrane protein pore  $\alpha$ -HL downstream of the promoter, transmembrane  $\alpha$ -HL pores could be generated after light activation. Using lipid coated aqueous droplets in oil as synthetic cells, the diffusion of dyes between droplets was realized through pores formed by light activation. Electrical communication was demonstrated by measuring ionic currents between droplets after the illumination of light. Furthermore, the authors printed synthetic tissues which contain hundreds of droplets with 3D printing similar to their previous work.<sup>44</sup> Light-activated electric communication was shown in 3D-printed pathways of synthetic tissues, which provided a primitive mimic of neuronal transmission.

With a different light responsive molecule, *trans-cis* photoisomerisation of azobenzene was implemented to tune the phase separation of coacervate droplets.<sup>48</sup> Coacervate droplets were formed by the electrostatic and hydrophobic interaction between azobenzene molecules and DNA. Upon UV activation, the droplets disassembled due to a lower affinity of *cis*-azobenzene with DNA. The reverse re-assembly of droplets could be realized under blue light or thermal relaxation in the dark. Following this principle, transfer, mixing and hybridization were shown in binary communities of droplets.

**3.1.2 Temperature.** By rational design, Mann and colleagues managed to use temperature to control the mechanochemical transduction of enzyme cascade reactions in prototissue spheroids (Fig. 7B).<sup>49</sup> The well-known thermoresponsive polymer, PNIPAM, was selected as building blocks of polymers for temperature responsiveness. The microscale prototissue spheroids were composed of bio-orthogonally linked protein-polymer microcapsules (proteinosomes) through alkyne-azide cycloaddition reaction. The resulted spheroids were able to contract and expand in a reversible and collective manner when transitioned above and below the lower critical solution temperature of polymers. The permeability of the spheroids was decreased in contracted state at higher temperature. The difference in permeability of spheroids was employed to sense the surrounding chemical signals and perform enzyme cascade reactions. To give a demonstration, glucose oxidase and horseradish peroxidase were trapped in binary populations of proteinosomes inside the thermoresponsive spheroids. In relaxed state at low temperature, substrates diffused freely through the spheroids and enzyme cascade reacted at a relatively high rate. As the temperature increased to induce the contraction of spheroids, diffusion of substrates was hindered, and the reaction rate of enzymes was decreased. This provided a rudimentary form of mechanochemical transduction of synthetic prototissues mediated by temperature.

**3.1.3 Chemical addition.** An artificial phagocytosis was reported in a binary community of synthetic protocells with chemical addition (Fig. 7C).<sup>50</sup> Silica colloidosomes could be engulfed by larger magnetic Pickering emulsion (MPE) droplets through an aperture in the droplets after the addition of oleic acid. The membrane of MPE droplets consisted of oleate-capped magnetite particles which would be destabilized after adding oleic acid molecules. Magnetite particles redistributed and magnetite-free apertures formed due to the

decreased interfacial tension of the adsorptive oleate anions at the surface of MPE droplets. The reduced interfacial tension as well as the possible assembly of bilayer on the colloidosome surface was responsible for the phagocytosis of colloidosomes into droplets. With this artificial phagocytosis behavior, the authors were able to demonstrate the delivery of payloads from colloidosomes to droplets after the engulfment. Fluorescence could be generated after the ingestion of colloidosomes followed by the enzyme mediated reaction.

Recently the authors extended this approach to achieve higher-order communication behaviors with enzyme-mediated reactions (Fig. 7D).<sup>51</sup> Once the catalase filled colloidosomes were engulfed by the  $H_2O_2$  containing MPE droplets, buoyant motion of the droplet was immediately activated due to the production of oxygen bubbles. Instead of adding chemical addition to trigger the phagocytosis, the oleic acid could be generated through the lipase mediated hydrolysis of triolein in MPE droplets. Therefore, the lipase trapped colloidosomes showed a self-triggering phagocytosis behavior like the virus. Furthermore, loading the colloidosomes with alkaline phosphatase was able to induce supramolecular hydrogelation of amino acids inside the MPE droplets. Using this interesting phagocytosis behavior between two protocell communities, various types of high-order communication were demonstrated.

### 3.2 Others

In addition to the stimuli triggered communication between vesicles, other techniques have also been used for artificial communication. For example, optical tweezers could individually manipulate liposomes to form linear, square and pyramidal assemblies (Fig. 7E).<sup>52</sup> Double adhering bilayers were formed at the interface of liposomes above certain salt concentrations. Interestingly, closed-ended tethers which resemble lipid membrane nanotubes were discovered as one vesicle was pulled away from the other using optical tweezers. The tether could be stretched over hundreds of microns without breaking which provides possibility of communication between vesicles across large distances. As a demonstration of communication between vesicles,  $\alpha$ -HL was introduced to produce pores in the membranes of two attached vesicles. After selectively blocking pores exposed to the environment using cyclodextrin blockers, pores in the intermembrane region remained open because of the larger size of blocker than the intermembrane distance. The survived pores in the interface region allowed the diffusion of  $Ca^{2+}$  from one compartment to the other wherein fluorescence was detected by the  $Ca^{2+}$  sensitive dye.

Mann group developed a technique using acoustic standing wave to trap arrays of coacervate microdroplets. Two separated arrays of microdroplets were patterned spatially containing GOx and HRP respectively.<sup>53</sup> Through an internally produced signaling molecule,  $H_2O_2$ , these two communities were chemically coupled under a unidirectional supply of substrates of glucose and *o*-phenylenediamine. As a response, fluorescence was produced specifically in the HRP loaded population in a time- and position-dependent manner. The same method was further explored to trap liposomes producing micro-arrays of



vesicles from 1D rows to 2D square or triangular geometries (Fig. 7F).<sup>54</sup> A GOx/HRP cascade reaction was established inter-vesicles *via* the diffusion of signals through melittin pores. This signal transduction strategy was further expanded to co-trapped vesicles and living cells which induced killing of cancer cells and bacterial gene expression.

## 4. Non-covalent interaction mediated communication

Interaction could bring different unities spatially close enough to enable communicative behaviors between compartments. So far, several types of interactions have been employed to build the complex behaviors as in nature.

### 4.1 Electrostatic interaction

Mann and coworkers designed synthetic protocell communities showing predatory behaviors using electrostatic interaction (Fig. 8A).<sup>55</sup> Specifically, negatively charged protein-polymer microcapsules were lysed by protease in positively charged coacervates when the two different particles were electrostatically attracted with contact. Transfer of payloads from the prey proteinosomes to the predator coacervates was further demonstrated with dextran, DNA and platinum nanoparticles during the killing process. A limitation of this system lies in the selectiveness of the payloads. It was indicated that only payloads with negative charges could be transferred into the positively charged coacervates. Although still in rudimen-

tary, this work shows the possibility to design protocell consortia with complex collective behaviors.

Based on the similar mechanism with electrostatic interaction, the same group recently developed ternary protocell communities showing response-retaliation behavior (Fig. 8B).<sup>56</sup> In addition to the negatively charged proteinosomes (P) and positively charged predator coacervates (C<sub>K</sub>), the other pH-sensitive coacervates (C<sub>T</sub>) were introduced. Counter-attacking coacervates, C<sub>K</sub>, were initially dormant and adhered to P by electrostatic attraction. Proteinosomes were sensitive to protease degradation and were loaded with GOx. Triggered by the addition of glucose signal, a toxin (H<sup>+</sup>) was secreted through the hydrolysis of the product from the GOx mediated reaction. The decrease in pH disassembled C<sub>T</sub>, resulting in the release of encapsulated protease. Protease was further transferred and re-captured by C<sub>K</sub> followed by the lysis of P and termination of GOx activity. By the antagonistic interactions, the authors were able to achieve programmable tit-for-tat behaviors based on the feedback from different protocells.

Inspired by the previous proteinosomes, a positively charged and thermo-sensitive proteinosome was developed to interact with *E. coli* (Fig. 8C).<sup>57</sup> The proteinosomes were filled with acid-sensitive hydrogel crosslinked by Schiff base bonds where L-arginine was incorporated. *E. coli* showed high affinity with the surface of proteinosomes through a combination of hydrophobicity and electrostatic interaction. The acidic metabolized products of *E. coli* colonies triggered the release of loaded L-arginine leading to a high bactericidal activity. Interestingly, by controlling the ionic strength and temperature,

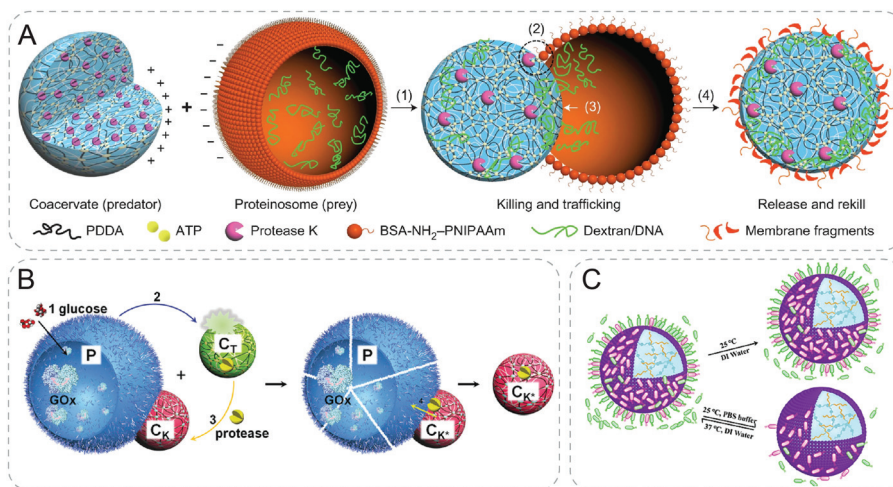


**Fig. 8** Communicative behaviors mediated by electrostatic interaction. (A) Artificial predator/prey behavior between synthetic communities. Assisted by electrostatic attraction, coacervate attracts and kills the prey, proteinosome, through protease-induced lysis of the membrane of prey, resulting in payloads transfer to the predator.<sup>55</sup> (B) Response-retaliation behavior in synthetic communities. Signal glucose is catalyzed by GOx-containing proteinosomes (P) to secrete H<sup>+</sup>, which disassembles pH-sensitive coacervate (C<sub>T</sub>). Encapsulated proteinase is then released from C<sub>T</sub> and re-concentrated by the other coacervate C<sub>K</sub> which is adsorbed on the surface of P electrostatically. As a result, P is ruptured by the proteolytic digestion, completing a tit-for-tat behavior.<sup>56</sup> (C) Modulation of the interaction of proteinosomes and bacteria by controlling the ionic strength (PBS buffer) and temperature.<sup>57</sup> Figures reproduced with permission from: (A), ref. 55, Copyright 2017 Springer Nature; (B), ref. 56, Copyright 2019 John Wiley and Sons; (C), ref. 57, Copyright 2020 Royal Society of Chemistry.



the proteinosomes could be renewed for a second use for killing *E. coli* by releasing the absorbed *E. coli* from the surface.

## 4.2 Specific complexation

Specific complexation such as antibody binding and avidin–biotin attraction was designed to demonstrate communication between synthetic vesicle and cell or between vesicles. Bentley group developed biological nanofactories using synthetic biology and biofabrication.<sup>58,59</sup> The self-assembled nanofactories were composed of a targeting antibody to bind the targeted bacteria, a sensing module to sense substrate and a synthetic module to synthesize and deliver the signaling molecule autoinducer-2. Delivery of autoinducer-2 was able to trigger a QS response from the other population of bacteria.<sup>58</sup> Therefore, the nanofactories were shown to act as a bridge to mediate the cell–cell communication. This strategy could be further extended to enable interspecies communication

between human epithelial cells and bacteria by modifying the module of the targeting antibody.<sup>59</sup>

Based on the previous reported transmembrane signaling transducer, vesicle and vesicle communication was realized by competitive avidin–biotin complexation (Fig. 9A).<sup>60</sup> The transducer was elaborately designed with two switchable headgroups. Under certain trigger, the external recognition headgroup was switched to be membrane permeable followed by the translocation across the bilayer of vesicle. Internal catalytic headgroup was activated to catalyze encapsulated substrate producing an output of fluorescent signal.<sup>61</sup> The competitive communication was realized by the transfer of avidin–desthiobiotin to avidin–biotin interaction which has a higher affinity. Transducer was anchored in the outer leaflet of liposomes due to the avidin–desthiobiotin complex. A second population of competitive liposomes displaying biotin would displace the avidin from the complex to set the transducer free to generate an output signal.

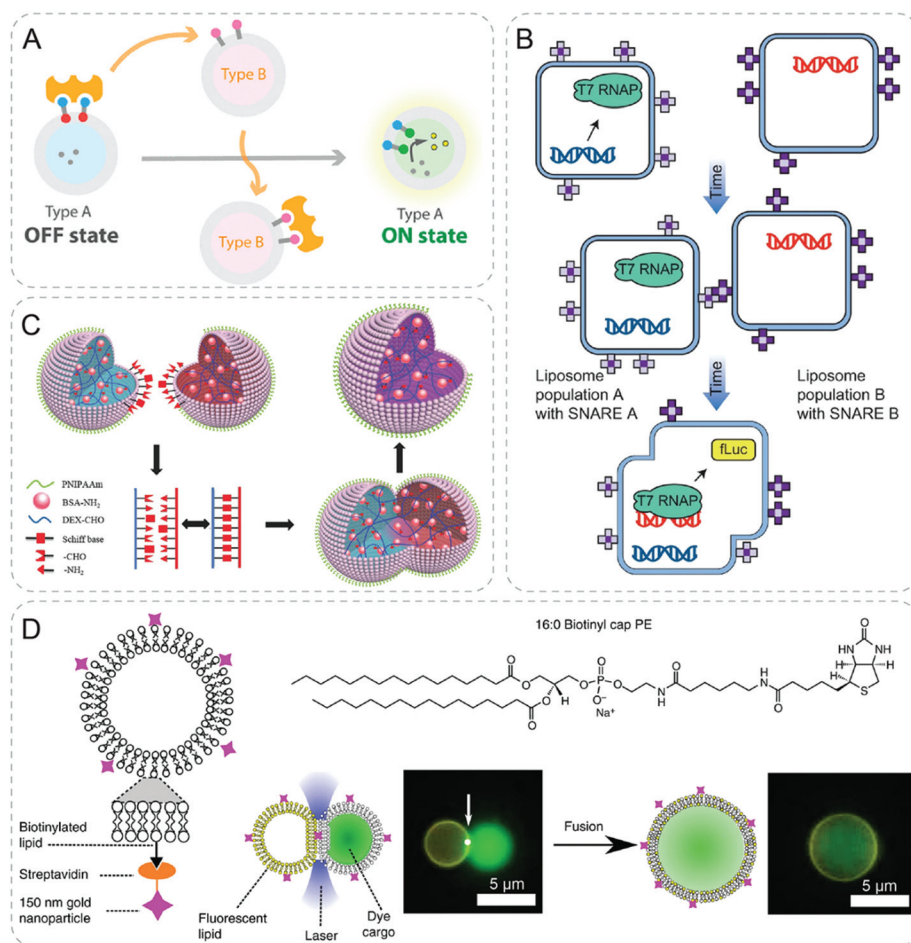


**Fig. 9** Communicative behaviors mediated by specific complexation or fusion. (A) Communication between vesicles by competitive avidin–biotin complexation. Type B vesicle takes away the avidin (yellow shape) from type A vesicle due to its higher binding affinity. The shift of avidin liberates the membrane-anchored transducer of type A and turns on its fluorescence.<sup>60</sup> (B) Liposome fusion induced by complementary protein (SNARE), resulting in hierarchical genetic circuits.<sup>40</sup> (C) Schiff base reaction induced fusion of two hydrogel proteinosomes upon contact generating a single larger proteinosome.<sup>62</sup> (D) Gold nanoparticle mediated fusion of liposomes with the application of laser.<sup>52</sup> Figures reproduced with permission from: (A), ref. 60, Copyright 2019 American Chemical Society; (B), ref. 40, Copyright 2017 Springer Nature; (C), ref. 62, Copyright 2017 John Wiley and Sons; (D), ref. 52, under a Creative Commons licence CC BY 4.0.



### 4.3 Fusion

With various kinds of fusing technology, vesicles of separate populations could be fused followed by subsequent reactions. Based on the same platform described in 2.1.2, genetic circuits in separate liposomes were brought together through the complementary protein induced fusion of liposomes (Fig. 9B).<sup>40</sup> With this strategy, one population first performed mammalian transcription. Subsequently, translation and protein production were achieved by fusing with the other population of liposomes, which are not compatible in the same compartment.

A different strategy to induce fusion of different compartments is shown by contact-induced fusion between vesicle and vesicle. Two hydrogel-filled proteinosomes fused by Schiff base reaction upon contact (Fig. 9C).<sup>62</sup> Single larger proteinosomes containing a mixture of payloads were obtained after the fusion. Furthermore, the fusion could happen between proteinosome and inorganic silica particles functionalized with amine resulting in encapsulation of intact silica particles inside.

Light-induced heat was also used to fuse the attached vesicles through optical tweezers as described previously (Fig. 9D).<sup>52</sup> Gold nanoparticles were attached on the surface of the liposomes. Under illumination of light, the nanoparticles would dissipate heat and cause fusion of vesicles. The fusion was localized to the spot being exposed to light, which could be used to perform sequential fusion of vesicles. Cell-free transcription and translation in three attached vesicles were realized after fusing the networks by light, leading to GFP synthesis.

## 5. Communication with active particles

As discussed in previous sections, most reported systems realizing artificial communication are based on passive particles, which is far away from the dynamic and out-of-equilibrium properties in nature. Individuals of different kingdoms at different scales are motile and far-away-from equilibrium by constant energy input. Meanwhile, signals for communication are often transmitted actively instead of solely passive diffusion. In this context, emerging field of research using inanimate but active micro- and nanoparticles shows great promise to emulate behaviors in living systems. To date, self-powered micro- and nanomotors have been shown surprising resemblance to natural behaviors, ranging from dynamic collective behaviors such as the flocking of birds to directional motion in gradients such as the chemotaxis.<sup>12,13,63</sup> Readers are referred to recent excellent reviews discussing collective behaviors of active particles for more information.<sup>64,65</sup> Here we highlight several representative examples showing complex collective behaviors and communication between individual active particles. Additionally, an emerging researching area using forces generated by active particles to dynamically deform the vesicle membrane will be briefly presented.

### 5.1 Collective behaviors

Collective behaviors of active particles could be controlled by external stimuli. In one example, light was used to activate colloidal particles leading to the assembly of living crystals from nonequilibrium forces (Fig. 10A).<sup>66</sup> Bi-material colloids were composed of polymer spheres encapsulating canted hematite cube which was partially exposed outside. In the solution of H<sub>2</sub>O<sub>2</sub> under blue light illumination, hematite catalyzes chemical decomposition of H<sub>2</sub>O<sub>2</sub> generating chemical gradients. The self-propelled motors showed dynamic self-assembly into crystals which can actively translate, rotate, collide, join and split due to the competition between self-propulsion and attraction resulted from phoresis and osmosis. These forces, *i.e.* the dynamic self-assembly of active particles, could be reversibly turned on and off by light.

Using electricity as a different stimulus, a variety of dynamic and collective states were shown in Janus particles (Fig. 10B).<sup>67</sup> Specifically, silica microspheres were hemispherically coated with titanium followed by a thin layer of SiO<sub>2</sub> for a homogeneous chemical surface. A.C. electric fields were applied to polarize metal and silica hemispheres differently. The resulting electrostatic imbalance of two hemispheres drove the propulsion of particles under the mechanism of induced-charge electrophoresis. This electrostatic imbalance resulted from differential dielectric responses was further responsible for the dipolar interaction among the active particles. Importantly, the dielectric responses were frequency dependent. Therefore, the collective behaviors could be easily tuned by changing the electric-field frequency. At low frequency of electric field, particles move and collide isotropically in a gas state showing negligible dipolar interactions. Increasing frequency to a moderate range, dipolar interactions were strong enough to cause the interaction between particles. Simultaneously, the swimming direction of particles was reversed toward the side of metal. The repulsion between metallic hemispheres aligned the particles producing coherent swarms. When the frequency was at megahertz range, particle chains were formed due to head-to-tail attraction arising from the opposite dipoles of the metallic and dielectric hemispheres. Addition of salt could tune the dipolar interaction forming clusters of particles. Furthermore, intriguing large-scale polar waves, vortices and clustering process were observed from swarm states in a time evolution manner.

### 5.2 Communication between individuals

Although collective behaviors are interesting and have been achieved in different systems, communicative behaviors in active particles are still not fully explored. To name a few examples, Solovev *et al.* described a primitive form of communication between two individual micromotors and a swarm.<sup>64</sup> The oxygen bubbles generated through the decomposition of H<sub>2</sub>O<sub>2</sub> of the two individuals were attracted to the swarm due to chemophoresis and capillary forces. Although



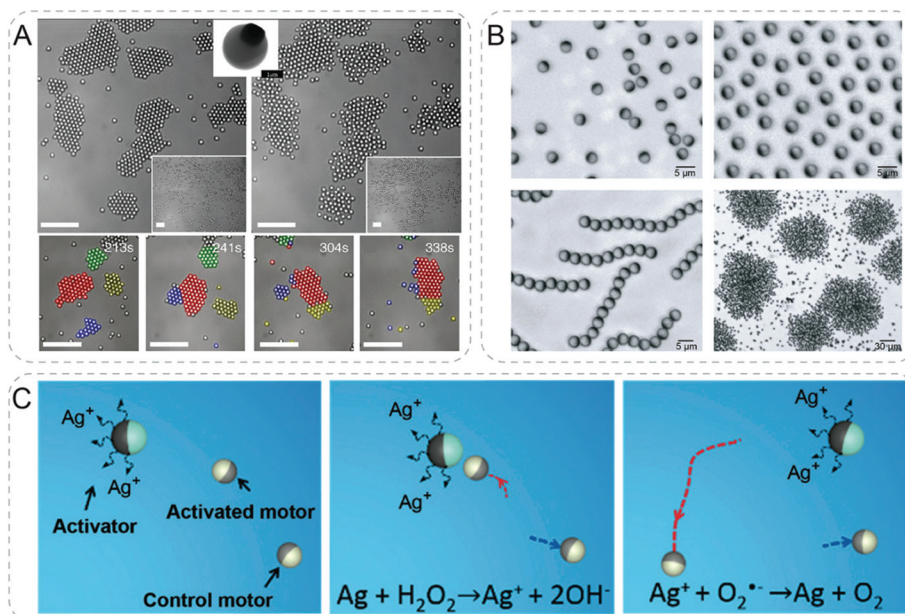


**Fig. 10** Communicative behaviors based on active particles. (A) Polymer/hematite Janus colloids reversibly assemble and disassemble with and without the illumination of blue light (top). The self-propelled active particles dynamically translate, rotate, collide, join and split due to the competition between self-propulsion and attraction resulted from phoresis and osmosis (bottom). All scale bars are 10  $\mu\text{m}$ .<sup>66</sup> (B) Janus colloids with differential dielectric responses form a series of collective behaviors by changing the electric-field frequency, including isotropic gases, swarms, chains, and clusters.<sup>67</sup> (C) Chemical communication between individual active motors. Because of the silver corrosion in  $\text{H}_2\text{O}_2$  medium, activator (polystyrene/Ni/Au/Ag motor) releases  $\text{Ag}^+$  ions, which are further reduced to Ag and deposited on the Pt surface of  $\text{SiO}_2/\text{Pt}$  activated motor. The resultant Ag/Pt bimetallic surface possess a significantly higher catalytic ability to decompose  $\text{H}_2\text{O}_2$ , thus increasing its speed.<sup>68</sup> Figures reproduced with permission from: (A), ref. 66, Copyright 2013 AAAS; (B), ref. 67, Copyright 2016 Springer Nature; (C), ref. 68, Copyright 2018 John Wiley and Sons.

the signal being transferred was not functional in communication, the authors showed the possibility to achieve interaction between active particles.

Recently, Wang group reported communication between individual active motors with chemical signals (Fig. 10C).<sup>68</sup> An activator motor sent chemical signal of  $\text{Ag}^+$  ions to a nearby receiver motor which dramatically increased its speed as a response. Two kinds of Janus motors self-propelled by decomposing the  $\text{H}_2\text{O}_2$  fuel to generate  $\text{O}_2$  molecules.  $\text{Ag}^+$  ions were released spontaneously from the surface of activator motor composed of polystyrene/Ni/Au/Ag due to silver corrosion in  $\text{H}_2\text{O}_2$  solution. In close proximity to an activator motor,  $\text{Ag}^+$  ions deposited on the Pt surface of the activated  $\text{SiO}_2/\text{Pt}$  motor. The formation of a bimetallic Ag/Pt structure with higher catalytic activity for  $\text{H}_2\text{O}_2$  decomposition resulted in accelerated motion of the activated motor. This work showed communication between synthetic particles in a dynamic context.

Adopting a similar principle, Zhou *et al.* demonstrated a one-way communication between active particles (termed micromotors) in which non-oscillatory micromotors learned to oscillate from oscillating Ag micromotors.<sup>69</sup> In this work,  $\text{Ag}^+$  was released from Ag micromotors during the oscillation and diffused onto the surface of Au–Rh rods. The accumulation of a small amount of Ag significantly increased the speed of Au–Rh micromotors.

### 5.3 Active forces

In contrast to thermodynamic forces exerted by passive particles, active particles bring propelling forces which have recently been employed to investigate dynamics of vesicle membrane both experimentally and theoretically in 2D and 3D.<sup>70–74</sup> Confined within vesicles, active forces generated by the motion of particles were shown to generate local curvature of the vesicle membrane. The induced curvature was further increased because of the accumulation of more particles, resulting in a positive feedback. Subsequently, morphologies of vesicles were evolved from simple circular (2D) and spherical (3D) to more complex and dynamic shapes, such as prolate and stomatocyte.<sup>70,72,74</sup> Similar phenomenon was recently reproduced in a bacteria-encapsulated vesicle model, where the active forces of the motion of bacteria drove nonequilibrium fluctuations and protruding tubes of the membrane.<sup>71</sup> Although the field of using the active forces generated by self-propelled particles is just emerging, more exciting findings are expected in the near future. For instance, the dynamic shape transformation of vesicles induced by active forces is reminiscent of the morphological transition of living cells induced by active forces as generated by microtubule filaments.<sup>70</sup> While the membrane tubes protruded by the propulsive bacterial forces share similarity with the process in mammalian cell infected by pathogens based on actin motility.<sup>71</sup>





## 6. Conclusion and future perspectives

Establishing communicative behaviors leveraging synthetic particles is an ambitious yet formidable goal. Reproducing the complex communication based on synthetic platforms brings us closer to passing the imitation game for a living artificial cell.<sup>75</sup> Relying on diverse principles as reviewed here, various artificial communicative behaviors have been shown. Diffusion of signal molecules from sender to receiver followed by a response of the receiver is reminiscent of the most common type of communication in bacterial colonies or multicellular eukaryotes. The generation of pores offers a solution to bypass the low permeability of the sender's membrane, therefore broadening the selection of both the signal molecules and the materials of synthetic particles. The concern of a lack of control in diffusion-mediated communication could be alleviated when the communication is regulated by external measures or non-covalent interaction between entities. Furthermore, complex communicative behaviors, such as phagocytosis and tit-for-tat, have also been achieved.

In spite of the significant endeavors in building communication on top of synthetic particles, the complexity of natural communication is still beyond the grasp of scientific scope. Communication as shown to date mostly follows the route of the initiation of signal transmission from sender to receiver following by a response of the receiver. This is principally quite close to the paradigm of intelligent drug delivery system.<sup>76</sup> For instance, responsive drug delivery carrier accumulates at targeting cancer sites through specific interaction. Upon receiving a signal externally such as light, ultrasound or *in situ* signals such as low pH from the cancer cells, delivery carrier degraded and cargoes were released to kill the cells. More advanced designs are required to fulfill interaction of a higher extent. Moreover, communication reported nowadays is mainly limited in a one-way level with only a few exceptions.<sup>25,26,34,35</sup> Reciprocal communication in nature is still far more superior to artificial ones with multiple feedbacks among different entities, leading to collective behaviors or homeostasis.

Signal diffusion of passive particles unsurprisingly suffers from a slow stochastic process with random directions. The consequence of such defects is the requirement of vicinity of particles or extra interaction such as electrostatic attraction to enable the diffusion of signals. From this point of view, active particles possess the potential to shift the stochastic diffusion of signal to a directed way because of the motion or chemical gradients created by catalytic reactions. The out-of-equilibrium state by constant energy influx can potentially lead to the development of more complex communicative behaviors. Notably, several recent studies with elaborate designs shed light on programable motion of active particles, ranging from visual-perception induced group behaviors, switchable fusion-fission transition, to controllable 3D helical trajectories.<sup>77–80</sup> This concept opens new avenues in enabling active particles to perform complex tasks through adaption and reconfiguration.

Despite the fact that significant margins are still present in order to emulate the communication in living world, tremendous developments exemplified in the current review advance the state of the art closer to the benchmark in nature. This endeavor will not only provide fresh impetus for advanced synthetic particles as artificial cells, but also aid the development of therapeutic applications in biomedical fields. For instance, synthetic particles possessing communicative abilities with living cells can be used as sentinels that could detect abnormal molecular signals and set off alarm signals. To play an active role, communicative synthetic particles are envisioned to bring more exciting progress in activating the immune system, regulating metabolism or even reprogramming cells.

## Conflicts of interest

There are no conflicts to declare.

## Acknowledgements

The authors acknowledge the NWO Chemische Wetenschappen VIDI grant 723.015.001 for financial support. We also acknowledge support from the Ministry of Education, Culture and Science (gravitation program 024.001.035).

## References

- 1 C. M. Waters and B. L. Bassler, *Annu. Rev. Cell Dev. Biol.*, 2005, **21**, 319–346.
- 2 S. D. Leonhardt, F. Menzel, V. Nehring and T. Schmitt, *Cell*, 2016, **164**, 1277–1287.
- 3 P. A. Brennan and F. Zufall, *Nature*, 2006, **444**, 308–315.
- 4 H. Youk and W. A. Lim, *Science*, 2014, **343**, 1242782.
- 5 M. T. Chen and R. Weiss, *Nat. Biotechnol.*, 2005, **23**, 1551–1555.
- 6 L. Schukur, B. Geering, G. Charpin-El Hamri and M. Fussenegger, *Sci. Transl. Med.*, 2015, **7**, 318ra201.
- 7 R. Lentini, N. Yeh Martín and S. S. Mansy, *Curr. Opin. Chem. Biol.*, 2016, **34**, 53–61.
- 8 E. Rideau, R. Dimova, P. Schwille, F. R. Wurm and K. Landfester, *Chem. Soc. Rev.*, 2018, **47**, 8572–8610.
- 9 W. Li, L. Zhang, X. Ge, B. Xu, W. Zhang, L. Qu, C. H. Choi, J. Xu, A. Zhang, H. Lee and D. A. Weitz, *Chem. Soc. Rev.*, 2018, **47**, 5646–5683.
- 10 F. Peng, Y. Tu and D. A. Wilson, *Chem. Soc. Rev.*, 2017, **46**, 5289–5310.
- 11 Y. Tu, F. Peng and D. A. Wilson, *Adv. Mater.*, 2017, **29**, 1701970.
- 12 M. You, C. Chen, L. Xu, F. Mou and J. Guan, *Acc. Chem. Res.*, 2018, **51**, 3006–3014.
- 13 I. Ortiz-Rivera, M. Mathesh and D. A. Wilson, *Acc. Chem. Res.*, 2018, **51**, 1891–1900.
- 14 X. Wei, M. Beltran-Gastelum, E. Karshalev, B. Esteban-Fernandez de Avila, J. Zhou, D. Ran, P. Angsantikul,



- R. H. Fang, J. Wang and L. Zhang, *Nano Lett.*, 2019, **19**, 1914–1921.
- 15 L. Kong, N. F. Rosli, H. L. Chia, J. Guan and M. Pumera, *Bull. Chem. Soc. Jpn.*, 2019, **92**, 1754–1758.
- 16 M. Godoy-Gallardo, M. J. York-Duran and L. Hosta-Rigau, *Adv. Healthcare Mater.*, 2018, **7**, 1700917.
- 17 A. Kuchler, M. Yoshimoto, S. Luginbuhl, F. Mavelli and P. Walde, *Nat. Nanotechnol.*, 2016, **11**, 409–420.
- 18 A. E. Nel, L. Madler, D. Velegol, T. Xia, E. M. Hoek, P. Somasundaran, F. Klaessig, V. Castranova and M. Thompson, *Nat. Mater.*, 2009, **8**, 543–557.
- 19 G. Rampioni, F. D'Angelo, L. Leoni and P. Stano, *Front. Bioeng. Biotechnol.*, 2019, **7**, 1.
- 20 L. Aufinger and F. C. Simmel, *Chem. – Eur. J.*, 2019, **25**, 12659–12670.
- 21 P. Stano, G. Rampioni, P. Carrara, L. Damiano, L. Leoni and P. L. Luisi, *BioSystems*, 2012, **109**, 24–34.
- 22 L. Wang, S. Song, J. van Hest, L. Abdelmohsen, X. Huang and S. Sanchez, *Small*, 2020, **16**, 1907680.
- 23 S. Sun, M. Li, F. Dong, S. Wang, L. Tian and S. Mann, *Small*, 2016, **12**, 1920–1927.
- 24 C. Arya, H. Oh and S. R. Raghavan, *ACS Appl. Mater. Interfaces*, 2016, **8**, 29688–29695.
- 25 A. Llopis-Lorente, P. Díez, A. Sánchez, M. D. Marcos, F. Sancenón, P. Martínez-Ruiz, R. Villalonga and R. Martínez-Mañez, *Nat. Commun.*, 2017, **8**, 15511.
- 26 B. de Luis, A. Llopis-Lorente, P. Rincon, J. Gadea, F. Sancenón, E. Aznar, R. Villalonga, J. R. Murguía and R. Martínez-Mañez, *Angew. Chem., Int. Ed.*, 2019, **58**, 14986–14990.
- 27 A. Ultimo, C. de la Torre, C. Giménez, E. Aznar, C. Coll, M. D. Marcos, J. R. Murguía, R. Martínez-Mañez and F. Sancenón, *Chem. Commun.*, 2020, **56**, 7273–7276.
- 28 M. Weitz, A. Muckl, K. Kapsner, R. Berg, A. Meyer and F. C. Simmel, *J. Am. Chem. Soc.*, 2014, **136**, 72–75.
- 29 G. Rampioni, F. D'Angelo, M. Messina, A. Zennaro, Y. Kuruma, D. Tofani, L. Leoni and P. Stano, *Chem. Commun.*, 2018, **54**, 2090–2093.
- 30 A. X. Lu, H. Oh, J. L. Terrell, W. E. Bentley and S. R. Raghavan, *Chem. Sci.*, 2017, **8**, 6893–6903.
- 31 H. Niederholtmeyer, C. Chagga and N. K. Devaraj, *Nat. Commun.*, 2018, **9**, 5027.
- 32 G. Gines, A. S. Zadorin, J. C. Galas, T. Fujii, A. Estevez-Torres and Y. Rondelez, *Nat. Nanotechnol.*, 2017, **12**, 351–359.
- 33 A. Joesaar, S. Yang, B. Bogels, A. van der Linden, P. Pieters, B. Kumar, N. Dalchau, A. Phillips, S. Mann and T. F. A. de Greef, *Nat. Nanotechnol.*, 2019, **14**, 369–378.
- 34 R. Lentini, N. Y. Martin, M. Forlin, L. Belmonte, J. Fontana, M. Cornella, L. Martini, S. Tamburini, W. E. Bentley, O. Jousson and S. S. Mansy, *ACS Cent. Sci.*, 2017, **3**, 117–123.
- 35 Y. Ding, L. E. Contreras-Llano, E. Morris, M. Mao and C. Tan, *ACS Appl. Mater. Interfaces*, 2018, **10**, 30137–30146.
- 36 J. A. Brophy and C. A. Voigt, *Nat. Methods*, 2014, **11**, 508–520.
- 37 E. Magdalena Estirado, A. F. Mason, M. Á. Alemán García, J. C. M. van Hest and L. Brunsveld, *J. Am. Chem. Soc.*, 2020, **142**, 9106–9111.
- 38 T. D. Tang, D. Cecchi, G. Fracasso, D. Accardi, A. Coutable-Pennarun, S. S. Mansy, A. W. Perriman, J. L. R. Anderson and S. Mann, *ACS Synth. Biol.*, 2018, **7**, 339–346.
- 39 Y. Elani, R. V. Law and O. Ces, *Nat. Commun.*, 2014, **5**, 5305.
- 40 K. P. Adamala, D. A. Martin-Alarcon, K. R. Guthrie-Honea and E. S. Boyden, *Nat. Chem.*, 2017, **9**, 431–439.
- 41 A. Dupin and F. C. Simmel, *Nat. Chem.*, 2019, **11**, 32–39.
- 42 R. Lentini, S. P. Santero, F. Chizzolini, D. Cecchi, J. Fontana, M. Marchioretto, C. Del Bianco, J. L. Terrell, A. C. Spencer, L. Martini, M. Forlin, M. Assfalg, M. Dalla Serra, W. E. Bentley and S. S. Mansy, *Nat. Commun.*, 2014, **5**, 4012.
- 43 P. M. Gardner, K. Winzer and B. G. Davis, *Nat. Chem.*, 2009, **1**, 377–383.
- 44 G. Villar, A. D. Graham and H. Bayley, *Science*, 2013, **340**, 48–52.
- 45 J. W. Hindley, D. G. Zheleva, Y. Elani, K. Charalambous, L. M. C. Barter, P. J. Booth, C. L. Bevan, R. V. Law and O. Ces, *Proc. Natl. Acad. Sci. U. S. A.*, 2019, **116**, 16711–16716.
- 46 G. J. T. Cooper and L. Cronin, *Nat. Chem.*, 2009, **1**, 342–343.
- 47 M. J. Booth, V. R. Schild, A. D. Graham, S. N. Olof and H. Bayley, *Sci. Adv.*, 2016, **2**, e1600056.
- 48 N. Martin, L. Tian, D. Spencer, A. Coutable-Pennarun, J. L. R. Anderson and S. Mann, *Angew. Chem., Int. Ed.*, 2019, **58**, 14594–14598.
- 49 P. Gobbo, A. J. Patil, M. Li, R. Harniman, W. H. Briscoe and S. Mann, *Nat. Mater.*, 2018, **17**, 1145–1153.
- 50 L. Rodríguez-Arco, M. Li and S. Mann, *Nat. Mater.*, 2017, **16**, 857–863.
- 51 L. Rodríguez-Arco, B. V. V. S. P. Kumar, M. Li, A. J. Patil and S. Mann, *Angew. Chem., Int. Ed.*, 2019, **58**, 6333–6337.
- 52 G. Bolognesi, M. S. Friddin, A. Salehi-Reyhani, N. E. Barlow, N. J. Brooks, O. Ces and Y. Elani, *Nat. Commun.*, 2018, **9**, 1882.
- 53 L. Tian, M. Li, J. Liu, A. J. Patil, B. W. Drinkwater and S. Mann, *ACS Cent. Sci.*, 2018, **4**, 1551–1558.
- 54 X. Wang, L. Tian, H. Du, M. Li, W. Mu, B. W. Drinkwater, X. Han and S. Mann, *Chem. Sci.*, 2019, **10**, 9446–9453.
- 55 Y. Qiao, M. Li, R. Booth and S. Mann, *Nat. Chem.*, 2017, **9**, 110–119.
- 56 Y. Qiao, M. Li, D. Qiu and S. Mann, *Angew. Chem., Int. Ed.*, 2019, **58**, 17758–17763.
- 57 C. Zhao, M. Zhu, Y. Fang, X. Liu, L. Wang, D. Chen and X. Huang, *Mater. Horiz.*, 2020, **7**, 157–163.
- 58 R. Fernandes, V. Roy, H. C. Wu and W. E. Bentley, *Nat. Nanotechnol.*, 2010, **5**, 213–217.
- 59 C. G. Hebert, A. Gupta, R. Fernandes, C.-Y. Tsao, J. J. Valdes and W. E. Bentley, *ACS Nano*, 2010, **4**, 6923–6931.
- 60 Y. Ding, N. H. Williams and C. A. Hunter, *J. Am. Chem. Soc.*, 2019, **141**, 17847–17853.
- 61 M. J. Langton, F. Keymeulen, M. Ciaccia, N. H. Williams and C. A. Hunter, *Nat. Chem.*, 2017, **9**, 426–430.



- 62 P. Wen, X. Liu, L. Wang, M. Li, Y. Huang, X. Huang and S. Mann, *Small*, 2017, **13**, 1700467.
- 63 L. Ren, W. Wang and T. E. Mallouk, *Acc. Chem. Res.*, 2018, **51**, 1948–1956.
- 64 A. A. Solovev, S. Sanchez and O. G. Schmidt, *Nanoscale*, 2013, **5**, 1284–1293.
- 65 H. Wang and M. Pumera, *Chem. Soc. Rev.*, 2020, **49**, 3211–3230.
- 66 J. Palacci, S. Sacanna, A. P. Steinberg, D. J. Pine and P. M. Chaikin, *Science*, 2013, **339**, 936–940.
- 67 J. Yan, M. Han, J. Zhang, C. Xu, E. Luijten and S. Granick, *Nat. Mater.*, 2016, **15**, 1095–1099.
- 68 C. Chen, X. Chang, H. Teymourian, D. E. Ramirez-Herrera, B. Esteban-Fernandez de Avila, X. Lu, J. Li, S. He, C. Fang, Y. Liang, F. Mou, J. Guan and J. Wang, *Angew. Chem., Int. Ed.*, 2018, **57**, 241–245.
- 69 C. Zhou, Q. Wang, X. Lv and W. Wang, *Chem. Commun.*, 2020, **56**, 6499–6502.
- 70 Y. Li and P. R. ten Wolde, *Phys. Rev. Lett.*, 2019, **123**, 148003.
- 71 S. C. Takatori and A. Sahu, *Phys. Rev. Lett.*, 2020, **124**, 158102.
- 72 H. R. Vutukuri, M. Hoore, C. Abaurrea-Velasco, L. van Buren, A. Dutto, T. Auth, D. A. Fedosov, G. Gompper and J. Vermant, 2019, arXiv preprint arXiv:1911.02381.
- 73 C. Wang, Y. K. Guo, W. D. Tian and K. Chen, *J. Chem. Phys.*, 2019, **150**, 044907.
- 74 M. Paoluzzi, R. Di Leonardo, M. C. Marchetti and L. Angelani, *Sci. Rep.*, 2016, **6**, 34146.
- 75 L. Cronin, N. Krasnogor, B. G. Davis, C. Alexander, N. Robertson, J. H. G. Steinke, S. L. M. Schroeder, A. N. Khlobystov, G. Cooper, P. M. Gardner, P. Siepmann, B. J. Whitaker and D. Marsh, *Nat. Biotechnol.*, 2006, **24**, 1203–1206.
- 76 Y. Wang and D. S. Kohane, *Nat. Rev. Mater.*, 2017, **2**, 17020.
- 77 F. A. Lavergne, H. Wendehenne, T. Bäuerle and C. Bechinger, *Science*, 2019, **364**, 70–74.
- 78 H. R. Vutukuri, M. Lisicki, E. Lauga and J. Vermant, *Nat. Commun.*, 2020, **11**, 2628.
- 79 J. G. Lee, A. M. Brooks, W. A. Shelton, K. J. M. Bishop and B. Bharti, *Nat. Commun.*, 2019, **10**, 2575.
- 80 M. A. Fernandez-Rodriguez, F. Grillo, L. Alvarez, M. Rathlef, I. Buttinoni, G. Volpe and L. Isa, *Nat. Commun.*, 2020, **11**, 4223.

